

 Open access • Journal Article • DOI:10.1063/1.3631087

## Phase-stabilization and substrate effects on nucleation and growth of (Ti,V) (n+1)GeC(n) thin films — [Source link](#)

[Sit Kerdsonpanya](#), [Kristina Buchholt](#), [Olof Tengstrand](#), [Jun Lu](#) ...+3 more authors

**Published on:** 12 Sep 2011 - [Journal of Applied Physics](#) (American Institute of Physics (AIP))

Related papers:

- [The Mn+1AXn phases: Materials science and thin-film processing](#)
- [The MN+1AXN phases: A new class of solids](#)
- [Generalized Gradient Approximation Made Simple](#)
- [Experimental and theoretical characterization of ordered MAX phases Mo2TiAlC2 and Mo2Ti2AlC3](#)
- [Projector augmented-wave method](#)

Share this paper:    

View more about this paper here: <https://typeset.io/papers/phase-stabilization-and-substrate-effects-on-nucleation-and-nnam8h3ecq>

# Phase-stabilization and substrate effects on nucleation and growth of $(\text{Ti},\text{V})(n+1)\text{GeC}(n)$ thin films

Sit Kerdsonpanya, Kristina Buchholt, Olof Tengstrand, Jun Lu,  
Jens Jensen, Lars Hultman and Per Eklund

**Linköping University Post Print**

N.B.: When citing this work, cite the original article.

Original Publication:

Sit Kerdsonpanya, Kristina Buchholt, Olof Tengstrand, Jun Lu, Jens Jensen, Lars Hultman and Per Eklund, Phase-stabilization and substrate effects on nucleation and growth of  $(\text{Ti},\text{V})(n+1)\text{GeC}(n)$  thin films, 2011, Journal of Applied Physics, (110), 5, 053516.

<http://dx.doi.org/10.1063/1.3631087>

Copyright: American Institute of Physics (AIP)

<http://www.aip.org/>

Postprint available at: Linköping University Electronic Press

<http://urn.kb.se/resolve?urn=urn:nbn:se:liu:diva-71221>

## Phase-stabilization and substrate effects on nucleation and growth of $(\text{Ti,V})_{n+1}\text{GeC}_n$ thin films

Sit Kerdsonpanya, Kristina Buchholt, Olof Tengstrand, Jun Lu, Jens Jensen et al.

Citation: *J. Appl. Phys.* **110**, 053516 (2011); doi: 10.1063/1.3631087

View online: <http://dx.doi.org/10.1063/1.3631087>

View Table of Contents: <http://jap.aip.org/resource/1/JAPIAU/v110/i5>

Published by the [American Institute of Physics](#).

---

### Related Articles

Role of interfacial transition layers in  $\text{VO}_2/\text{Al}_2\text{O}_3$  heterostructures

*J. Appl. Phys.* **110**, 073515 (2011)

Effects of stress on the optical properties of epitaxial Nd-doped  $\text{Sr}_{0.5}\text{Ba}_{0.5}\text{Nb}_2\text{O}_6$  films

*AIP Advances* **1**, 032172 (2011)

Polycrystalline iron nitride films fabricated by reactive facing-target sputtering: Structure, magnetic and electrical transport properties

*J. Appl. Phys.* **110**, 053911 (2011)

Growth of a crystalline and ultrathin MgO film on  $\text{Fe}(001)$

*AIP Advances* **1**, 032156 (2011)

Structural and magnetic properties of quaternary  $\text{Co}_2\text{Mn}_{1-x}\text{Cr}_x\text{Si}$  Heusler alloy thin films

*J. Appl. Phys.* **110**, 053903 (2011)

---

### Additional information on *J. Appl. Phys.*

Journal Homepage: <http://jap.aip.org/>

Journal Information: [http://jap.aip.org/about/about\\_the\\_journal](http://jap.aip.org/about/about_the_journal)

Top downloads: [http://jap.aip.org/features/most\\_downloaded](http://jap.aip.org/features/most_downloaded)

Information for Authors: <http://jap.aip.org/authors>

### ADVERTISEMENT

**AIPAdvances**

*Submit Now*

**Explore AIP's new  
open-access journal**

- **Article-level metrics  
now available**
- **Join the conversation!  
Rate & comment on articles**

## Phase-stabilization and substrate effects on nucleation and growth of $(\text{Ti,V})_{n+1}\text{GeC}_n$ thin films

Sit Kerdsonpanya,<sup>a)</sup> Kristina Buchholt, Olof Tengstrand, Jun Lu, Jens Jensen, Lars Hultman, and Per Eklund

*Thin Film Physics Division, Department of Physics, Chemistry, and Biology, IFM, Linköping University, SE-581 83 Linköping, Sweden*

(Received 16 June 2011; accepted 26 July 2011; published online 12 September 2011)

Phase-pure epitaxial thin films of  $(\text{Ti,V})_2\text{GeC}$  have been grown onto  $\text{Al}_2\text{O}_3(0001)$  substrates via magnetron sputtering. The  $c$  lattice parameter is determined to be 12.59 Å, corresponding to a 50/50 Ti/V solid solution according to Vegard's law, and the overall  $(\text{Ti,V})\text{:Ge:C}$  composition is 2:1:1 as determined by elastic recoil detection analysis. The minimum temperature for the growth of  $(\text{Ti,V})_2\text{GeC}$  is 700 °C, which is the same as for  $\text{Ti}_2\text{GeC}$  but higher than that required for  $\text{V}_2\text{GeC}$  (450 °C). Reduced Ge content yields films containing  $(\text{Ti,V})_3\text{GeC}_2$  and  $(\text{Ti,V})_4\text{GeC}_3$ . These results show that the previously unknown phases  $\text{V}_3\text{GeC}_2$  and  $\text{V}_4\text{GeC}_3$  can be stabilized through alloying with Ti. For films grown on 4H-SiC(0001),  $(\text{Ti,V})_3\text{GeC}_2$  was observed as the dominant phase, showing that the nucleation and growth of  $(\text{Ti,V})_{n+1}\text{GeC}_n$  is affected by the choice of substrate; the proposed underlying physical mechanism is that differences in the local substrate temperature enhance surface diffusion and facilitate the growth of the higher-order phase  $(\text{Ti,V})_3\text{GeC}_2$  compared to  $(\text{Ti,V})_2\text{GeC}$ . © 2011 American Institute of Physics. [doi:10.1063/1.3631087]

### I. INTRODUCTION

The class of ternary nitrides and carbides known as  $\text{M}_{n+1}\text{AX}_n$  phases ( $n=1,2,3$ ) comprises compounds made of M (a transition metal); an element from groups 12–16 (A), usually group 13 or 14; and a third element, X, that is either nitrogen or carbon.<sup>1–3</sup> MAX phases are divided into three subgroups:  $\text{M}_2\text{AX}$ ,  $\text{M}_3\text{AX}_2$ , and  $\text{M}_4\text{AX}_3$ , or “211,” “312,” and “413” phases, respectively. Recently,  $(\text{Ti,Nb})_5\text{AlC}_4$ , the first example of a “514” phase, was discovered by Zheng *et al.*<sup>4</sup> The MAX phases' unusual anisotropic hexagonal nanolaminated structure give remarkable properties such as high resistance to thermal shock, machinability, ductility, and high thermal and electrical conductivity.<sup>1,2</sup>

Among the research topics related to MAX phases, solid solutions are interesting because the effect of chemistry on synthesis, phase stability, and properties can be studied.<sup>3,5</sup> These solid solutions can be categorized in three groups: (i) M-site solutions  $(\text{M}_1\text{M}_2)_{n+1}\text{AX}_n$ , (ii) A-site solid solutions  $\text{M}_{n+1}(\text{A}_1\text{A}_2)\text{X}_n$ , and (iii) X-site solutions  $\text{M}_{n+1}\text{A}(\text{X}_1\text{X}_2)_n$ .<sup>2</sup> Different MAX-phase solid solutions have been investigated as bulk materials (e.g., Refs. 1, 5–9). However, solid solution MAX-phase thin films have been studied much less and offer an important opportunity for exploration, as it is relatively easy to grow MAX phases epitaxially,<sup>10–16</sup> and thin-film growth permits the study of materials that are metastable and difficult to synthesize in bulk.<sup>2</sup> Among the relatively few studies that exist on MAX-phase solid solutions in thin films, Scarbozi *et al.* reported M-site solid solutions of  $(\text{Ti,Nb})_2\text{AlC}$  thin films.<sup>17</sup> From Raman scattering, they indirectly determined the elastic modulus, suggesting solid solution hardening. Furthermore, in thin films, the oxycarbide X-site solid

solution  $\text{Ti}_2\text{Al}(\text{C,O})$  has been reported as a result of the incorporation of oxygen from the residual gas in a vacuum deposition process<sup>18</sup> or due to a reaction between TiC or  $\text{Ti}_2\text{AlC}$  layers with an  $\text{Al}_2\text{O}_3$  substrate.<sup>19,20</sup>

Here, we investigate the Ti-V-Ge-C system. The end members  $\text{Ti}_2\text{GeC}$  and  $\text{V}_2\text{GeC}$  exist in bulk<sup>1,2</sup> and have also been grown as thin-film materials.<sup>14,21–25</sup> However, the two systems differ in that the Ti-Ge-C system contains two other MAX phases ( $\text{Ti}_3\text{GeC}_2$  and  $\text{Ti}_4\text{GeC}_3$ ),<sup>2,24</sup> whereas the V-Ge-C system does not contain them, and in that the lowest reported growth temperature required in order to form  $\text{Ti}_2\text{GeC}$  is  $\sim 700$  °C ( $\sim 800$  °C for phase-pure  $\text{Ti}_2\text{GeC}$ ), whereas  $\text{V}_2\text{GeC}$  can be grown at temperatures down to  $\sim 450$  °C. The Ti-V-Ge-C system is therefore an ideal model system for investigating whether the “312” and “413” phases can be stabilized in the V-Ge-C system by alloying with Ti, and for determining whether the growth temperature of  $(\text{Ti,V})_2\text{GeC}$  can be substantially reduced compared to that of  $\text{Ti}_2\text{GeC}$ .

### II. EXPERIMENTAL DETAILS

The  $(\text{Ti,V})_2\text{GeC}$  thin films were deposited using dc magnetron sputtering in an ultrahigh vacuum chamber (base pressure lower than  $10^{-7}$  Pa) in an Ar (99.9999%) discharge at a pressure of  $\sim 0.5$  Pa. Three targets were used for the depositions: Ti/V (50 at. %/50 at. %, 99.9% purity), Ge (99.99% purity), and graphite (99.99% purity), with diameters of 75, 50, and 75 mm, respectively. The targets were operated in current-control mode with (Ti,V) at 310 mA ( $\sim 311$  V), Ge at 50 to 70 mA ( $\sim 333$ – $340$  V), and C at 370 to 400 mA ( $\sim 630$ – $722$  V). The substrate temperature ( $T_s$ ) was varied in the range of 350–800 °C. Details about the deposition system can be found elsewhere.<sup>10</sup>

The substrates were  $(12.5 \times 12.5)$  mm<sup>2</sup> of  $\text{Al}_2\text{O}_3(0001)$ , single-side polished, and a 4H-SiC(0001)  $n$ -type wafer,

<sup>a)</sup>Author to whom correspondence should be addressed. Electronic mail: sitke@ifm.liu.se.

Si-face, cut  $4^\circ$  off-axis, from SiCrystal.<sup>26</sup> The 4H-SiC(0001) substrate has a  $1\ \mu\text{m}$  thick  $p$ - ( $4 \times 10^{15}\ \text{cm}^{-3}$ ) doped epitaxially grown SiC layer with a  $0.8\ \mu\text{m}$   $n$ - ( $1.5 \times 10^{19}\ \text{cm}^{-3}$ ) doped epitaxially grown SiC layer on top. The dopant atoms used for the epilayers were Al and N for the  $p$ - and  $n$ -type, respectively, and were grown at the Institute Acreo.<sup>27</sup> Prior to deposition, the substrates were ultrasonically degreased in two steps—in acetone for 5 min and isopropanol for 5 min—and blown dry in  $\text{N}_2$ , inserted into the chamber, and thermally degassed at the substrate temperature for 1 h. 4H-SiC substrates were plasma etched for 30 min to remove any surface oxides on the 4H-SiC (as in Ref. 28).

The structural characterization of as-deposited films was performed via x-ray diffraction (XRD)  $\theta$ - $2\theta$  scans using Cu  $K_\alpha$  as an x-ray source with a Philips PW 1820 diffractometer. The (0004) 4H-SiC was aligned at an offset of  $\sim 4^\circ$ , because the 4H-SiC substrate is cut  $4^\circ$  off-axis. A Leo 1550 Gemini scanning electron microscope (SEM) with an accelerating voltage of 5 kV was used to study the surface morphology with secondary-electron images. A Dimension 3100 atomic force microscope (AFM) was also used to investigate the surface morphology. Transmission electron microscope (TEM) cross-sectional samples were prepared via mechanical polishing followed by ion milling in a Gatan Precision Ion Polishing System using argon ions with an energy of 5 keV, with a final polishing step at 2 keV. The TEM was an FEI Tecnai G2 TF 20 UT with a field-emission gun operated at an acceleration voltage of 200 keV. Time-of-flight elastic recoil detection analysis (ERDA) was applied in order to obtain the elemental depth profiles of the as-deposited films. The measurements were performed with a 40 MeV  $^{127}\text{I}^{9+}$  ion beam using the set-up at Uppsala University.<sup>29,30</sup> The recoil angle was  $45^\circ$ , with both the incident angle of primary ions and the exit angle of recoils set to  $67.5^\circ$  relative to the surface normal. All spectra were analyzed using the CONTEC code,<sup>31</sup> with which the recoil energy of each element was converted to relative atomic concentration profiles.

Nanoindentation was performed on a film  $\sim 1\ \mu\text{m}$  in thickness with a Berkovich diamond tip at room temperature. The Oliver and Pharr method<sup>32</sup> was used to calculate the hardness ( $H$ ) and the reduced Young's modulus ( $E_r$ ). Twenty-seven indents were made at a force of 2.6 mN. The indentation depth was around  $0.09\ \mu\text{m}$ . The stated error bars correspond to the standard deviation in the obtained  $H$  and  $E_r$  values. Additional control measurements with varied forces were made, and no substantial differences in  $H$  and  $E_r$  were seen.

### III. RESULTS AND DISCUSSION

Figure 1 shows a  $\theta$ - $2\theta$  x-ray diffractogram of a Ti/V-Ge-C film deposited at a Ti/V current of 310 mA ( $\sim 311\ \text{V}$ ), a Ge current of 60 mA ( $\sim 340\ \text{V}$ ), a C current of 370 mA ( $\sim 660\ \text{V}$ ), and a substrate temperature ( $T_s$ ) =  $800^\circ\text{C}$  on an  $\text{Al}_2\text{O}_3$  substrate. Diffraction peaks are observed at  $2\theta$  angles of  $14.09^\circ$ ,  $28.37^\circ$ , and  $43.09^\circ$ . For pure  $\text{Ti}_2\text{GeC}$ , the 0002, 0004, and 0006 peaks are at  $2\theta$  angles of  $13.69^\circ$ ,  $27.57^\circ$ , and  $41.89^\circ$ , respectively (ICDD PDF 89-2278); these peaks for  $\text{V}_2\text{GeC}$  are at  $14.45^\circ$ ,  $29.14^\circ$ , and  $44.33^\circ$  (ICDD PDF

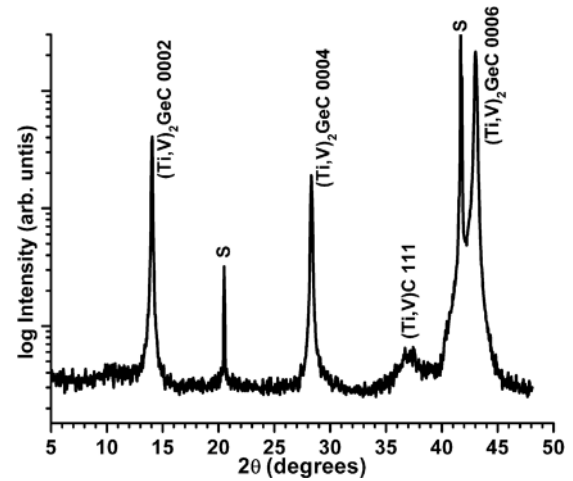


FIG. 1. X-ray diffractogram of phase-pure  $(\text{Ti,V})_2\text{GeC}$  films deposited onto an  $\text{Al}_2\text{O}_3(0001)$  substrate (marked by “S” in the diffractogram) at a substrate temperature of  $800^\circ\text{C}$ . The targets were operated at 310 mA (Ti/V), 60 mA (Ge), and 370 mA (C).

89-2276). The diffraction peaks from the Ti/V-Ge-C film are between the nominal positions for  $\text{Ti}_2\text{GeC}$  and  $\text{V}_2\text{GeC}$ , showing that this film is a virtually phase-pure solid solution of  $(\text{Ti,V})_2\text{GeC}$ . The broad, low-intensity peak from  $(\text{Ti,V})\text{C}$  at  $\sim 36.7^\circ$  mainly comes from an incubation layer formed at the initial stage of nucleation, similar to what has been observed for  $\text{Ti}_3\text{SiC}_2$ .<sup>10</sup> In addition, trace amounts of  $(\text{Ti,V})\text{C}$  in the film were observed in TEM as inclusions (not shown). The  $c$  lattice parameter of  $(\text{Ti,V})_2\text{GeC}$  determined from the XRD peak positions is  $12.59\ \text{\AA}$ , which is between the  $c$  lattice parameters of  $\text{Ti}_2\text{GeC}$  ( $c = 12.93\ \text{\AA}$ ) and  $\text{V}_2\text{GeC}$  ( $c = 12.25\ \text{\AA}$ ). Assuming that Vegard's law holds, the Ti/V ratio determined from these lattice parameters is 50/50, i.e., the same composition as in the Ti/V target.

Figure 2 shows  $\theta$ - $2\theta$  XRD patterns of Ti/V-Ge-C films deposited onto  $\text{Al}_2\text{O}_3(0001)$  with the same deposition

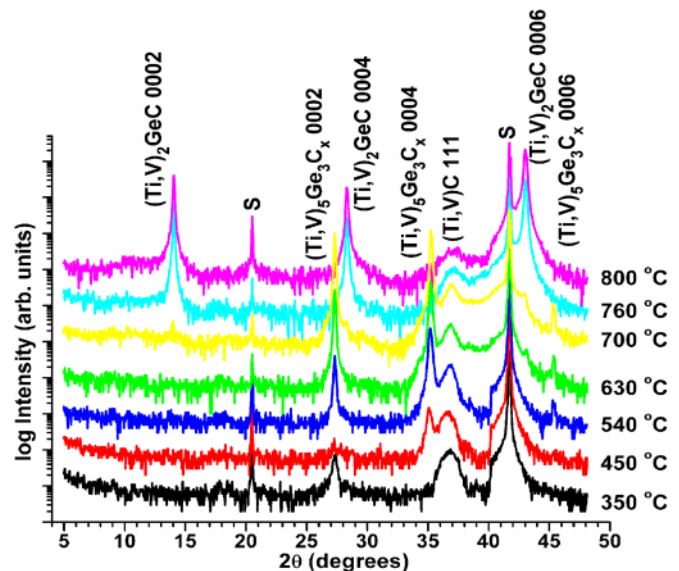


FIG. 2. (Color online) X-ray diffractograms of Ti/V-Ge-C films deposited onto  $\text{Al}_2\text{O}_3(0001)$  substrate (S). The targets were operated at 310 mA (Ti/V), 60 mA (Ge), and 370 mA (C). The substrate temperature is varied from  $350^\circ\text{C}$  to  $800^\circ\text{C}$ . The  $T_s = 800^\circ\text{C}$  scan is taken from Fig. 1.



parameters as in Fig. 1, except that  $T_s$  was varied from 350 °C to 800 °C. For  $T_s = 350$  °C, the (Ti,V)C peak is strong. For higher  $T_s$ , the peak intensity of (Ti,V)C decreases, and at  $T_s = 700$  °C, the (Ti,V)<sub>2</sub>GeC is present. There are additional peaks at  $2\theta$  angles of 27.3°, 35.5°, and 46.2°, respectively, that can be attributed to (Ti,V)<sub>5</sub>Ge<sub>3</sub>C<sub>x</sub> (the peak positions are between Ti<sub>5</sub>Ge<sub>3</sub>C<sub>x</sub> and V<sub>5</sub>Ge<sub>3</sub>C<sub>x</sub>).<sup>24,25</sup> Also, at  $T_s = 700$  °C, the (Ti,V)<sub>5</sub>Ge<sub>3</sub>C<sub>x</sub> and (Ti,V)C peaks are strong, and (Ti,V)<sub>2</sub>GeC is present as a minority phase. For  $T_s = 760$  °C, the (Ti,V)<sub>5</sub>Ge<sub>3</sub>C<sub>x</sub> peaks are not present and the (Ti,V)C peak becomes smaller, whereas (Ti,V)<sub>2</sub>GeC shows a high intensity. The films consist of phase-pure solid-solution (Ti,V)<sub>2</sub>GeC at  $T_s = 800$  °C, except for the trace amounts of (Ti,V)C mentioned above (see Fig. 1).

Table I shows the composition (determined by ERDA) of the Ti/V-Ge-C films in Fig. 2. The phase-pure (Ti,V)<sub>2</sub>GeC film grown at  $T_s = 800$  °C (Fig. 1) has a composition of (Ti,V)<sub>0.525</sub>Ge<sub>0.244</sub>C<sub>0.221</sub>, or 2:1:1 within the error bars of this technique. ERDA does not permit the separation of the Ti and V signals; however, according to the application of Vegard's law to the XRD results (see above), the Ti/V ratio is 50/50. We can thus conclude that the phase-pure solid solution film has (Ti<sub>0.5</sub>V<sub>0.5</sub>)<sub>2</sub>GeC stoichiometry.

As mentioned, the lowest reported substrate temperature of Ti<sub>2</sub>GeC is ~700 °C (~800 °C for phase-pure Ti<sub>2</sub>GeC), whereas V<sub>2</sub>GeC can be grown at temperatures down to ~450 °C. Our results show that the lowest possible substrate temperature for (Ti<sub>0.5</sub>V<sub>0.5</sub>)<sub>2</sub>GeC does not largely differ from that of Ti<sub>2</sub>GeC, i.e., films deposited at 700 °C contain (Ti<sub>0.5</sub>V<sub>0.5</sub>)<sub>2</sub>GeC, whereas ~800 °C is required for phase-pure (Ti<sub>0.5</sub>V<sub>0.5</sub>)<sub>2</sub>GeC. This is surprising because, in general, the substrate temperature for MAX phases is lower for transition metals (M) from groups 5 and 6 in the periodic table.<sup>2,24,25,33–36</sup> As previously reviewed,<sup>2</sup> the M–C bonding energy generally decreases going from group 4 to group 6 (e.g., from Ti to Cr), and kinetics should therefore favor M and C diffusion in MAX phases, with group 5 and 6 transition metals (e.g., V and Cr) requiring lower substrate temperatures for these MAX phases than the ones with group 4 transition metals. Our results indicate that this effect is not substantial for a 50/50 Ti/V mixture and that diffusion is not enhanced compared to the pure Ti-Ge-C system. A possible reason for this result could be that the (Ti,V)C and (Ti,V)<sub>5</sub>Ge<sub>3</sub>C<sub>x</sub> phase with smaller unit cells are favorably formed at these kinetically limited conditions, as is the case for the Ti-Ge-C system.<sup>24</sup>

Figure 3 shows x-ray diffractograms of Ti/V-Ge-C films deposited on Al<sub>2</sub>O<sub>3</sub>(0001) at  $T_s = 800$  °C. Table II shows the composition (determined by ERDA) of the films in Fig. 3.

TABLE I. Composition of the Ti/V-Ge-C films in Fig. 2 (determined by ERDA).

$T_s$ (°C)	350	450	540	700	760	800
(Ti,V) content (at. %)	46.4	47.1	46.3	50.6	51.7	52.5
Ge content (at. %)	30.4	28.8	28.2	24.4	24.1	24.7
C content (at. %)	22.9	22.1	22.5	23.5	24.1	22.1
O content (at. %)	0.3	2.0	3.0	1.5	0.1	0.7

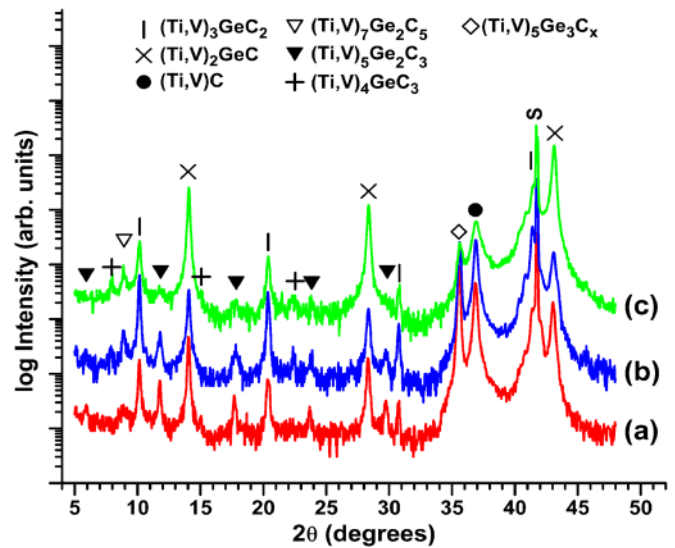


FIG. 3. (Color online) X-ray diffractograms of phase-mixed Ti/V-Ge-C MAX phase films deposited onto Al<sub>2</sub>O<sub>3</sub>(0001) substrate (S) at a substrate temperature of 800 °C. The targets were operated at (a) 310 mA (Ti/V), 55 mA (Ge), and 370 mA (C); (b) 310 mA (Ti/V), 55 mA (Ge), and 400 mA (C); and (c) 310 mA (Ti/V), 70 mA (Ge), and 400 mA (C).

Film (a), deposited under a Ti/V current of 310 mA, a Ge current of 55 mA, and a C current of 370 mA, exhibits XRD peaks at  $2\theta$  angles of 10.16°, 20.36°, 30.76°, and 41.38°. These peaks correspond to the 0002, 0004, 0006, and 0008 peaks of (Ti,V)<sub>3</sub>GeC<sub>2</sub>. From the XRD results, the  $c$  lattice parameter of this 312 phase is 17.42 Å. This film also shows peaks originating from (Ti,V)<sub>5</sub>Ge<sub>2</sub>C<sub>3</sub>, a “523” phase that can be described as intergrown alternating half-unit cells of 211 and 312 phases.<sup>2,23,24,37</sup> For the film in Fig. 3(b), the C target current is increased from 370 mA to 400 mA. The XRD pattern shows increased “312” content relative to “211.” Figure 3(c) shows the XRD of a film deposited at a higher Ge flux (changed from 55 mA to 70 mA). As expected, the amount of Ge-rich phases (“211” and “53x”) increases relative to the Ge-poor phases. Furthermore, in Figs. 3(a)–3(c), minute peaks are observed at  $2\theta$  angles of 7.88° and 15.04°, which correspond to a small amount of (Ti,V)<sub>4</sub>GeC<sub>3</sub>. There is also diffraction from (Ti,V)<sub>7</sub>Ge<sub>2</sub>C<sub>5</sub>, a “725” phase with intergrown alternating half-unit cells of 413 and 312 phases.<sup>38</sup>

Our results (Fig. 3) show that a reduction in Ge content, compared to the phase-pure (Ti,V)<sub>2</sub>GeC, results in the formation of (Ti,V)<sub>3</sub>GeC<sub>2</sub> and small amounts of (Ti,V)<sub>4</sub>GeC<sub>3</sub>. The hypothetical phases V<sub>3</sub>GeC<sub>2</sub> and V<sub>4</sub>GeC<sub>3</sub> can thus be partially stabilized via alloying with Ti. Furthermore, it is expected that fluctuations in the local Ge growth flux can

TABLE II. Composition of the Ti/V-Ge-C films in Fig. 3 and Fig. 4 (determined by ERDA).

Film	Target current (mA)			$T_s$ (°C)	Composition (at. %)			
	Ti/V	Ge	C		Ti/V	Ge	C	O
a	310	55	370	800	56.7	17.0	26.0	0.3
b	310	55	400	800	54.4	16.5	28.6	0.5
c	310	70	400	800	52.3	18.0	29.6	0.1

result in mixtures of 211, 312, and 413 phases. This explains the observations of “523” and “725” intergrown phases, which are known from the Ti-Ge-C system but not the V-Ge-C system.<sup>2,24</sup> In the binary V-C system, there are binary carbide superstructures such as  $V_8C_7$  that might prevent the formation of 312 and 413 phases. Apparently, there is a higher tendency to form  $V_2GeC$  with binary-carbide inclusions when growth fluctuations occur,<sup>25</sup> which might explain this difference between  $(Ti_{0.5}V_{0.5})_2GeC$  and  $V_2GeC$ .

Figure 4 shows XRD patterns of Ti/V-Ge-C films deposited on (a) 4H-SiC(0001) and (b)  $Al_2O_3(0001)$  substrates using identical growth conditions (Ti/V current of 310 mA ( $\sim 301$  V), Ge current of 80 mA ( $\sim 330$  V), C current of 370 mA ( $\sim 720$  V), and  $T_s = 800$  °C) in the same deposition batch in geometrically equivalent positions in the rotating substrate holder. The XRD results (Fig. 4(a)) show that the film deposited onto  $Al_2O_3(0001)$  is a “211”-“523”-“312” phase-mixture. In contrast, the Ti/V-Ge-C film grown on 4H-SiC(0001) exhibits a dominant  $(Ti,V)_3GeC_2$  phase with only minor amounts of  $(Ti,V)_2GeC$ . The ERDA results for this film showed that the overall composition is 51.7 at. % Ti/V, 16.7 at. % Ge, and 31.6 at. % C, or 3:1:2 within the accuracy of the technique. Because everything else is equal, these results show that the substrate affects the growth of Ti/V-Ge-C films. There is no epitaxial match by low integer number ratio between the *c*-axis height of  $(Ti,V)_3GeC_2$  and the step heights<sup>39,40</sup> on the 4H-SiC substrates; therefore, a direct effect of the epitaxy conditions on nucleation cannot explain this observation. The difference should rather be related to enhanced diffusion on 4H-SiC as compared to  $Al_2O_3$ . This is possible, because SiC is a far better thermal conductor than  $Al_2O_3$ , and the actual local surface temperature might be higher for the case of deposition onto SiC than for deposition onto  $Al_2O_3$ . This would favor the formation of the larger-unit-cell phase  $(Ti,V)_3GeC_2$ .

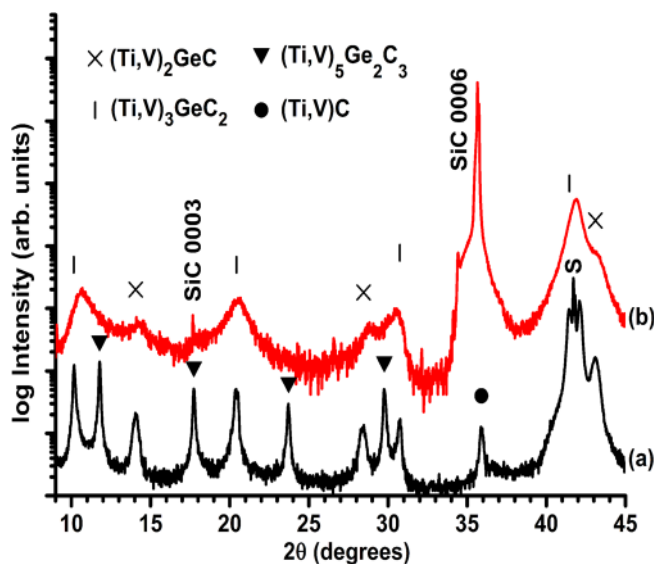


FIG. 4. (Color online) X-ray diffractograms of phase-mixed Ti/V-Ge-C MAX phase films deposited onto (a) 4H-SiC(0001) and (b)  $Al_2O_3(0001)$  substrates, with the  $Al_2O_3(0001)$  substrate peak indicated by “S.” Both films were grown at the same time. The targets were operated at 310 mA (Ti/V), 80 mA (Ge), and 370 mA (C). The substrate temperature was kept at 800 °C.

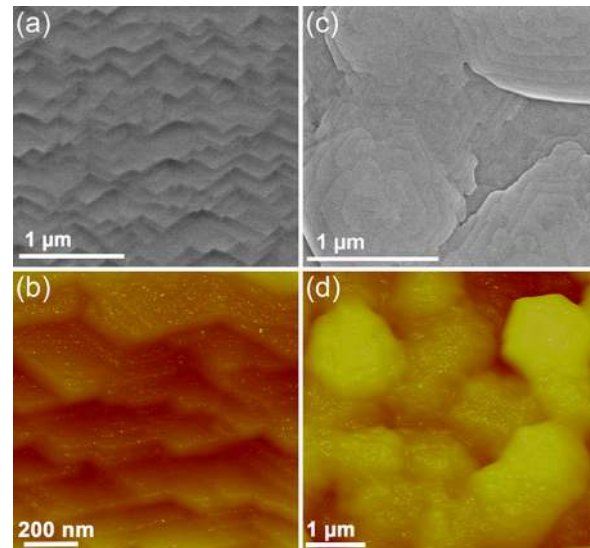


FIG. 5. (Color online) SEM and AFM images of phase mixed Ti/V-Ge-C MAX phase films with different substrates (a),(b) on 4H-SiC(0001) and (c),(d) on  $Al_2O_3(0001)$ .

Figures 5(a) and 5(b) show SEM and AFM images, respectively, of the surface morphology of the phase mixed Ti/V-Ge-C film on 4H-SiC substrate. Both techniques show stacked layers with steps, which are of the  $\{11\bar{2}0\}$  family.<sup>41</sup> The off cut of the 4H-SiC substrate presents growth steps for the films generating the step-flow growth mode on the film (0001) surface, similar to  $Ti_3SiC_2$  films on 4H-SiC(0001).<sup>41</sup> However, the growth of  $Ti_3SiC_2$  films requires Si-supersaturated conditions in order to maintain the faceted steps,<sup>41</sup> whereas the supersaturated condition is not required for such growth of the Ti/V-Ge-C system. This might be due to the difference in the diffusivity of Si and Ge. However, the phase mixed Ti/V-Ge-C film on  $Al_2O_3$  substrate has a completely different surface morphology from the film grown on 4H-SiC [see the SEM and AFM images in Figs. 5(c) and 5(d), respectively]. The SEM image shows that the film has spiral-growth steps from threading screw dislocation. This growth mode has also been seen in the Ti-Si-C system.<sup>10</sup>

Figure 6 shows cross-sectional TEM images of the phase-mixed Ti/V-Ge-C MAX phase film on  $Al_2O_3(0001)$  grown under the same conditions as in Fig. 3(a). Figure 6(a) shows an overview, and Fig. 6(b) is a high-resolution TEM image showing the nanolaminated structure of  $(Ti,V)_2GeC$  with the *c* lattice parameter ( $c_{211}$ ) measured to 12.5 Å. The film also has regions of  $(Ti,V)_3GeC_2$  (Fig. 6(c)) where the *c* lattice parameter is measured ( $c_{312}$ ) to 17.4 Å. These values differ slightly from the more reliable values obtained from XRD, given the degree of error in the lattice parameter determination in TEM.

The hardness and reduced Young’s modulus were measured via nanoindentation for 1- $\mu$ m-thick phase-mixed (Ti,V)-Ge-C MAX-phase film (XRD pattern similar to Fig. 3(c)). The values obtained from nanoindentation are  $12.4 \pm 0.9$  GPa and  $241 \pm 15$  GPa, respectively. Our determined hardness values are considerably higher than the values measured on bulk polycrystalline MAX phase materials,

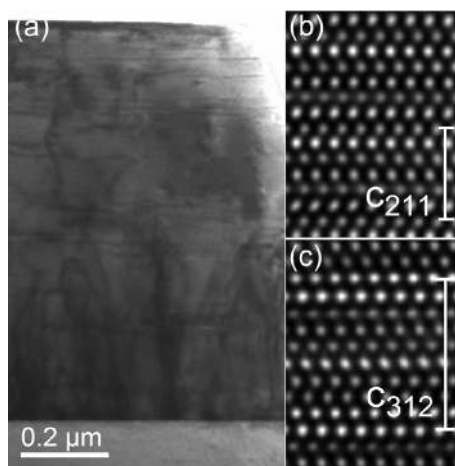


FIG. 6. Cross-sectional TEM images from a phase-mixed Ti/V-Ge-C film (a) in an overview, and (b),(c) high resolution images of 211 and 312 MAX phases. The lattice parameters  $c_{211}$  and  $c_{312}$  have lengths of 12.5 Å and 17.4 Å in (b) and (c), respectively.

which are around 2 to 5 GPa.<sup>1</sup> However, in thin films, the measured hardness values are typically higher because of indentation size effects and possible anisotropy effects.<sup>2</sup> Our measured hardness of  $12.4 \pm 0.9$  GPa is a rather typical number and does not indicate (or disprove) any solid solution hardening. In addition, small amounts of binary-carbide inclusions inside the film are known to affect the determination of mechanical properties,<sup>25,42</sup> which might also affect the present values.

#### IV. CONCLUSIONS

Phase-pure  $(\text{Ti}_{0.5}\text{V}_{0.5})_2\text{GeC}$  thin films can be grown using dc magnetron sputtering on  $\text{Al}_2\text{O}_3(0001)$  substrates at a substrate temperature of 800 °C. The  $c$  lattice parameter of  $(\text{Ti},\text{V})_2\text{GeC}$  is 12.59 Å, which is between those of  $\text{Ti}_2\text{GeC}$  ( $c = 12.93$  Å) and  $\text{V}_2\text{GeC}$  ( $c = 12.25$  Å). The Ti/V ratio determined from these lattice parameters is 50/50. The substrate temperature that is required for the epitaxial growth of  $(\text{Ti},\text{V})_2\text{GeC}$  is similar to that for  $\text{Ti}_2\text{GeC}$  ( $T_s = 700$  °C). The hypothetical phases  $\text{V}_3\text{GeC}_2$  and  $\text{V}_4\text{GeC}_3$  are realized by alloying with Ti. In contrast, Ti/V-Ge-C films grown on 4H-SiC under otherwise identical conditions have  $(\text{Ti},\text{V})_3\text{GeC}_2$  as the dominant phase; the suggested underlying mechanism is the difference in the local substrate temperatures of  $\text{Al}_2\text{O}_3$  and SiC, which enhances surface diffusion and facilitates the growth of the higher-order phase  $(\text{Ti},\text{V})_3\text{GeC}_2$  compared to  $(\text{Ti},\text{V})_2\text{GeC}$ .

#### ACKNOWLEDGMENTS

We acknowledge funding from the Swedish Research Council (VR) and the Swedish Agency for Innovation Systems (VINNOVA) Excellence Center FunMat. Dr. Jenny Frodelius is acknowledged for nanoindentation measurements.

<sup>1</sup>M. W. Barsoum, *Prog. Solid State Chem.* **28**, 201 (2000).

<sup>2</sup>P. Eklund, M. Beckers, U. Jansson, H. Högberg, and L. Hultman, *Thin Solid Films* **518**, 1851 (2010).

<sup>3</sup>J. Wang and Y. Zhou, *Annu. Rev. Mater. Res.* **39**, 415 (2009).

- <sup>4</sup>L. Zheng, J. Wang, X. Lu, F. Li, and Y. Zhou, *J. Am. Ceram. Soc.* **93**, 3068 (2010).
- <sup>5</sup>F. L. Meng, Y. C. Zhou, and J. Y. Wang, *Scr. Mater.* **53**, 1369 (2005).
- <sup>6</sup>N. A. Phatak, S. K. Saxena, Y. Fei, and J. Hu, *J. Alloys Compd.* **475**, 629 (2009).
- <sup>7</sup>I. Salama, T. El-Raghy, and M. W. Barsoum, *J. Alloys Compd.* **347**, 271 (2002).
- <sup>8</sup>J. Yi, P. Chena, D. Li, X. Xiao, W. Zhanga, and B. Tang, *Solid State Commun.* **150**, 49 (2010).
- <sup>9</sup>B. Manoun, S. K. Saxena, G. Huga, A. Ganguly, E. N. Hoffman, and M. W. Barsoum, *J. Appl. Phys.* **101**, 113523 (2007).
- <sup>10</sup>J. Emmerlich, H. Högberg, S. Sasvári, P. O. Å. Persson, L. Hultman, J. P. Palmquist, U. Jansson, J. M. Molina-Aldareguia, and Z. Czigány, *J. Appl. Phys.* **96**, 4817 (2004).
- <sup>11</sup>P. Eklund, A. Murugaiah, J. Emmerlich, Z. Czigány, J. Frodelius, M. W. Barsoum, H. Högberg, and L. Hultman, *J. Cryst. Growth* **304**, 264 (2007).
- <sup>12</sup>D. P. Sigumonrong, J. Zhang, Y. Zhou, D. Music, J. Emmerlich, J. Mayer, and J. M. Schneider, *Scr. Mater.* **64**, 347 (2011).
- <sup>13</sup>D. P. Sigumonrong, J. Zhang, Y. Zhou, D. Music, and J. M. Schneider, *J. Phys. D: Appl. Phys.* **42**, 185408 (2009).
- <sup>14</sup>J. Emmerlich, P. Eklund, D. Rittrich, H. Högberg, and L. Hultman, *J. Mater. Res.* **22**, 2279 (2007).
- <sup>15</sup>J. Frodelius, P. Eklund, M. Beckers, P. O. Å. Persson, H. Högberg, and L. Hultman, *Thin Solid Films* **518**, 1621 (2010).
- <sup>16</sup>M. D. Tucker, P. O. Å. Persson, M. C. Guenette, J. Rosén, M. M. M. Bilek, and D. R. McKenzie, *J. Appl. Phys.* **109**, 014903 (2011).
- <sup>17</sup>T. H. Scabarozzi, C. Gennaoui, J. Roche, T. Flemming, K. Wittenberger, P. Hann, B. Adamson, A. Rosenfeld, M. W. Barsoum, J. D. Hettinger, and S. E. Lofland, *Appl. Phys. Lett.* **95**, 101907 (2009).
- <sup>18</sup>J. Rosén, P. O. Å. Persson, M. Ionescu, A. Kondyurin, D. R. McKenzie, and M. M. M. Bilek, *Appl. Phys. Lett.* **92**, 064102 (2008).
- <sup>19</sup>O. Wilhelmsson, J. P. Palmquist, E. Lewin, J. Emmerlich, P. Eklund, P. O. Å. Persson, H. Högberg, S. Li, R. Ahuja, O. Eriksson, L. Hultman, and U. Jansson, *J. Cryst. Growth* **291**, 290 (2006).
- <sup>20</sup>P. O. Å. Persson, J. Rosén, D. R. McKenzie, M. M. M. Bilek, and C. Höglund, *J. Appl. Phys.* **103**, 066102 (2008).
- <sup>21</sup>M. Magnuson, O. Wilhelmsson, M. Mattesini, S. Li, R. Ahuja, O. Eriksson, H. Högberg, L. Hultman, and U. Jansson, *Phys. Rev. B* **78**, 035117 (2008).
- <sup>22</sup>T. H. Scabarozzi, P. Eklund, J. Emmerlich, H. Högberg, T. Meehan, P. Finkel, M. W. Barsoum, J. D. Hettinger, L. Hultman, and S. E. Lofland, *Solid State Commun.* **146**, 498 (2008).
- <sup>23</sup>H. Högberg, L. Hultman, J. Emmerlich, T. Joelsson, P. Eklund, J. M. Molina-Aldareguia, J.-P. Palmquist, O. Wilhelmsson, and U. Jansson, *Surf. Coat. Technol.* **193**, 6 (2005).
- <sup>24</sup>H. Högberg, P. Eklund, J. Emmerlich, J. Birch, and L. Hultman, *J. Mater. Res.* **20**, 779 (2005).
- <sup>25</sup>O. Wilhelmsson, P. Eklund, H. Högberg, L. Hultman, and U. Jansson, *Acta Mater.* **56**, 2563 (2008).
- <sup>26</sup>SiCrystal AG, Guenther-Scharowsky-Str.1, D 910 58 Erlangen, Germany.
- <sup>27</sup>More information about the Institute (Acreo AB, Electrum 239, 164 40 Kista, Sweden) can be found at <http://www.acreo.se/>.
- <sup>28</sup>K. Buchholt, R. Ghandi, M. Domeij, C. M. Zetterling, J. Lu, P. Eklund, L. Hultman, and A. L. Spetz, *Appl. Phys. Lett.* **98**, 042108 (2011).
- <sup>29</sup>H. J. Whitlow, G. Possnert, and C. S. Petersson, *Nucl. Instrum. Methods Phys. Res. B* **27**, 448 (1987).
- <sup>30</sup>J. Jensen, D. Martin, A. Surpi, and T. Kubart, *Nucl. Instrum. Methods Phys. Res. B* **268**, 1893 (2010).
- <sup>31</sup>M. S. Janson, "CONTES, Conversion of Time-Energy Spectra, a Program for ERDA Data Analysis," Internal Report, Uppsala University, 2004.
- <sup>32</sup>W. C. Oliver and G. M. Pharr, *J. Mater. Res.* **7**, 1564 (1992).
- <sup>33</sup>A. Abdulkadhim, M. to Baben, T. Takahashi, V. Schnabel, M. Hans, C. Polzer, P. Polcik, and J. M. Schneider, *Surf. Coat. Technol.* (in press).
- <sup>34</sup>J. J. Li, L. F. Hu, F. Z. Li, M. S. Li, and Y. C. Zhou, *Surf. Coat. Technol.* **204**, 3838 (2010).
- <sup>35</sup>Q. M. Wang, A. Flores Renteria, O. Schroeter, R. Mykhaylonka, C. Leyens, W. Garkas, and M. to Baben, *Surf. Coat. Technol.* **204**, 2343 (2010).
- <sup>36</sup>P. Eklund, M. Bugnet, V. Mauchamp, S. Dubois, C. Tromas, J. Jensen, L. Piroux, L. Gence, M. Jaouen, and T. Cabioc'h, *Phys. Rev. B* **84**, 075424 (2011).
- <sup>37</sup>J. P. Palmquist, S. Li, P. O. Å. Persson, J. Emmerlich, O. Wilhelmsson, H. Högberg, M. I. Katsnelson, B. Johansson, R. Ahuja, O. Eriksson, L. Hultman, and U. Jansson, *Phys. Rev. B* **70**, 165401 (2004).



- <sup>38</sup>T. H. Scabarozi, J. D. Hettinger, S. E. Lofland, J. Lu, L. Hultman, J. Jensen, and P. Eklund, *Scripta Mater.* (in press).
- <sup>39</sup>B. E. Landini and G. R. Brandes, *Appl. Phys. Lett.* **74**, 2632 (1999).
- <sup>40</sup>T. Kimoto, A. Itoh, and H. Matsunami, *Appl. Phys. Lett.* **66**, 3645 (1995).

- <sup>41</sup>K. Buchholt, P. Eklund, J. Jensen, J. Lu, A. Lloyd Spetz, and L. Hultman, *Scr. Mater.* **64**, 1141 (2011).
- <sup>42</sup>O. Wilhelmsson, P. Eklund, F. Giuliani, H. Hogberg, L. Hultman, and U. Jansson, *Appl. Phys. Lett.* **91**, 123124 (2007).